J. Fluid Mech. (1972), *vol.* 52, *part* 4, *pp.* 683–712
Printed in Great Britain

The effect of Brownian motion on the rheological properties of a suspension of non-spherical particles

By E. J. HINCH
Department of Applied Mathematics and Theoretical Physics, University of Cambridge
AND L. G. LEAL
Department of Chemical Engineering, California Institute of Technology

(Received 11 November 1971)

The effect of rotary Brownian motion on the rheology of a dilute suspension of rigid spheroids in shear flow is considered for various limiting cases of the particle aspect ratio r and dimensionless shear rate γ/D. As a preliminary the probability distribution function is calculated for the orientation of a single, axisymmetric particle in steady shear flow, assuming small particle Reynolds number. The result for the case of weak-shear flows, $\gamma/D \ll 1$, has been known for many years. After briefly reviewing this limiting case, we present expressions for the case of strong shear where $(r^3+r^{-3}) \ll \gamma/D$, and for an intermediate regime relevant for extreme aspect ratios where $1 \ll \gamma/D \ll (r^3+r^{-3})$. The bulk stress is then calculated for these cases, as well as the case of nearly spherical particles $r \sim 1$, which has not hitherto been discussed in detail. Various non-Newtonian features of the suspension rheology are discussed in terms of prior continuum mechanical and experimental results.

1. Introduction

In this paper we continue our earlier study (Leal & Hinch 1971) of the rheological effects of Brownian rotations in a dilute suspension of rigid spheroids. It proves convenient to consider the theoretical derivation of the bulk suspension properties in two parts. First, we consider the influence of the random Brownian couples on the creeping motion of the individual particles, for an assumed two-dimensional shear flow of the suspension. Second, the relationship between measurable bulk rheological properties and the microscale description of the suspension is deduced. This latter part of the problem has recently been throughly re-examined by Batchelor (1970). In this paper we focus our discussion on the microscale aspects of the rotary Brownian motion effects and on the qualitative features of the bulk stress.

The creeping motion of a small, rigid ellipsoid subjected to simple shear flow of a Newtonian fluid is described, in the *absence* of rotary Brownian motion,

by the now classical solution of Jeffery (1922). This solution shows that the particle will traverse any one of an infinite family of periodic closed orbits. As the particle geometry deviates from spherical, the angular velocity around any of these orbits becomes increasingly non-uniform with the particle tending to spend the major portion of every orbit period in a particular aligned position. The orbit for each particle is predicted to be unchanged for all time and hence to be determined by the particle's orientation at some initial time.

The action of rotary Brownian motion is a randomizing influence on the particle orientation so that the final distribution of orientations represents a compromise between the anisotropic distribution associated with the undisturbed Jeffery orbits and the uniform distribution which results from unopposed random Brownian couples. We observe that, under the influence of even the weakest rotary Brownian motion, the steady-state orientation distribution is independent of the initial orientation state.

The probability distribution function for particle orientation is governed by a modified Fokker–Planck equation. The formulation of this advection/diffusion equation in orientation space, reproduced in §2, can be traced back at least to Boeder (1932). However, he was unable to solve the full equation, and so simplified the problem to an ordinary differential equation by assuming that the particle orbit lay entirely in the plane perpendicular to the vorticity vector of the undisturbed shear flow. The first step in solving the full advective-diffusion equation came with the approximation scheme of Burgers (1938) for the case of strong Brownian motion. He computed the first few terms of an asymptotic expansion for the orientation distribution function, valid in the limit as the rotary Brownian diffusion coefficient D is large. The solution shows that the relatively weak shear flow causes little preferential alignment of the particle, i.e. there is only a small departure from the totally random state in which all orientations are equally probable. At nearly the same time, Peterlin (1938) obtained a solution for the orientation distribution function for near-spheres in terms of a slowly convergent series of spherical harmonics. He started with the uniform state, and based his expansion on the idea that for near-spheres the particle angular velocity is little different from the constant rotation of a sphere. Much later, Scheraga (1955) employed a digital computer in order to evaluate a very large number of terms in Peterlin's expansion. He calculated orientation-dependent angle averages for unrestricted aspect ratios, r, and values of γ/D ranging from zero to 200, where γ is the shear rate. The latter value of 200 essentially represented the limits of storage capacity for the computer. Other workers (Sadron 1953) obtained a representation for the case of near-spheres (§5*b*) which is unlimited with regard to the relative strength of the rotary Brownian motion. As will become evident, this expression allows an evaluation of the bulk rheological properties valid for any value of γ/D and hence provides an extremely useful case for comparison with the asymptotic expressions in which γ/D is assumed to be either very large or very small.

Much more recently, the case of weak rotary Brownian motion has been considered by Leal & Hinch (1971). In this limiting case, the particles proceed nearly undisturbed around closed Jeffery orbits. The first effect of the small Brownian

rotations is to eliminate the dependence, noted by Jeffery, of the relative population of different orbits on the initial orientation state of the suspension. By observing that, in the steady state, there was no *net* diffusion of particles out of an orbit Leal & Hinch (1971) derived an expression for the first approximation to the orientation distribution function, valid for sufficiently weak Brownian motion. The main feature of interest in this limiting case is the large departure from the uniform orientation state. In § 3, we develop expressions for the higher order approximations which are required for calculation of the full bulk stress tensor. A careful examination of the conditions under which this expansion is valid suggests the existence of a fourth regime corresponding to intermediate shear rates for particles with extreme aspect ratios. When the aspect ratio of the particles is either very large (rod-like) or very small (disk-like), we have already noted that the particles spend most of an undisturbed Jeffery orbit near a particular orientation. It is therefore possible for rotary Brownian diffusion to be negligible at *nearly* all orientations, but comparable with the shear (advection) in a small region about this one direction. In § 4, we derive an expression for the orientation distribution function for this intermediate regime by employing the methods of matched asymptotic expansions. In § 5, the full bulk stress tensor is determined from the calculated form of the microstructure for these limiting cases following the general procedure outlined by Batchelor (1970).

A complete set of references on the rheology of suspensions in the presence of Brownian rotations may be found in Brenner (1972), of which we draw special attention to the review papers of Sadron (1953), as well as the original works of Giesekus (1962) and Scheraga (1955). With the single exception of Giesekus's paper, however, these investigations have been solely concerned with calculations of the effective viscosity from the dissipation and hence, so far as we are aware, the case of strong rotary Brownian motion considered by Giesekus is the only one for which a complete evaluation of the bulk stress has been published. In this paper we have included a summary of results for the steady-state bulk stress tensor in four general asymptotic cases: that of strong rotary Brownian motion; of weak Brownian rotation; of the intermediate regime with extreme particle aspect ratios; and of nearly spherical particles with Brownian rotations of arbitrary strength. The first of these cases is essentially that of Giesekus (1962) and is presented, in a shortened version, mainly for completeness. The second and third are entirely new, with the exception of our previously reported work (Leal & Hinch 1971), and comprise the major contribution of the present paper. The near-sphere case is new only to the extent that the complete expressions for the bulk stress have not hitherto been published. As in the case of strong rotary Brownian motions, this near-sphere case is included mainly for the sake of completeness. Additionally, it is useful because it provides a check on the results of the other sections.

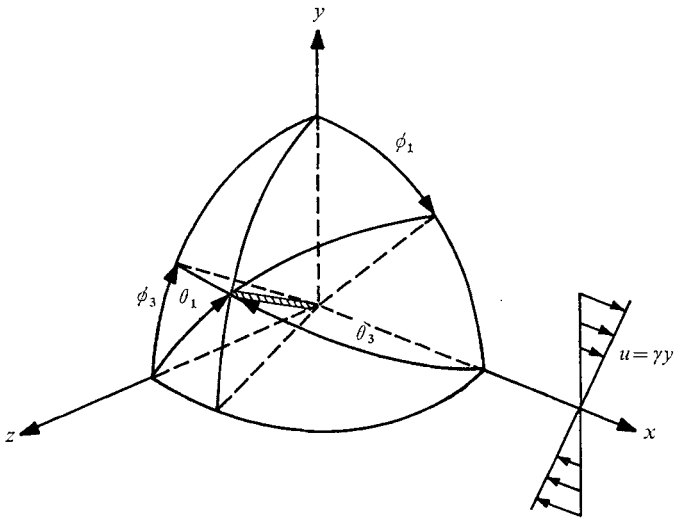

FIGURE 1. The polar angles.

2. General equations

(a) *The orientation distribution function*

We begin by considering a single neutrally buoyant, spheroidal particle suspended in an infinite incompressible Newtonian fluid which is undergoing a uniform shearing motion defined by

$$u = \gamma y; \quad v = w = 0. \tag{1}$$

Because of the symmetry of the particle, its orientation relative to a Cartesian co-ordinate system fixed at its centre is completely defined by the two polar angles θ_1, ϕ_1 of its axis of revolution as shown in figure 1. In the absence of inertial and Brownian motion effects, Jeffery (1922) has shown that the rotation of a spheroid with aspect ratio r is given by

$$\left.\begin{aligned} \dot{\phi}_1 &= \Omega + E\frac{r^2-1}{r^2+1}\cos 2\phi_1, \\ \dot{\theta}_1 &= \tfrac{1}{2}E\frac{r^2-1}{r^2+1}\sin 2\theta_1 \sin 2\phi_1, \end{aligned}\right\} \tag{2}$$

where for the simple shear flow (1) both the vorticity in the z direction, 2Ω, and twice the strain in the x, y plane, $2E$, are equal to the shear rate γ. Bretherton (1962) has observed that almost all axially symmetric particles will rotate according to (2) provided that r is replaced by an appropriate, effective aspect ratio.

To describe the statistics of a particle's orientation, we follow our previous paper (Leal & Hinch 1971, hereafter referred to as I) and introduce the differential probability density function $N(\theta_1, \phi_1)$ defined such that the probability of finding the particle with orientation in the interval $[\theta_1, \theta_1 + d\theta_1] \times [\phi_1, \phi_1 + d\phi_1]$ is $N(\theta_1, \phi_1) \sin\theta_1 d\theta_1 d\phi_1$. Then, as shown by Boeder (1932), Burgers (1938), and subsequently stated by us in I, the steady-state distribution of orientations is

governed by the advective-diffusion equation

$$\operatorname{div}(\gamma \mathbf{w} N) = D\nabla^2 N, \tag{3}$$

which simply expresses the conservation of probability in the orientation space. Here D is the rotational Brownian diffusion coefficient defined in I, and $\mathbf{w}$ is the vector

$$\gamma \mathbf{w} = (0, \dot{\theta}_1, \dot{\phi}_1 \sin\theta_1)$$

describing the time rate of change of orientation due to the *purely* hydrodynamic motion about Jeffrey orbits. The vector operators in (3) are, of course, defined on the unit sphere – the orientation space. The only additional conditions on N are the normalization

$$\int_0^{\pi} d\theta_1 \int_0^{2\pi} \sin\theta_1 \, d\phi_1 N(\theta_1, \phi_1) = 1 \tag{4}$$

plus the constraint that N be everywhere non-negative. The resulting probability function $N(\theta_1, \phi_1)$ depends essentially on two parameters – the particle aspect ratio r and the non-dimensional measure of the shear strength γ/D. We have outlined a number of solutions of the problem represented by (3) and (4) in the previous section, some of which are presented here for the first time, and some of which have been reported by previous investigators. We shall discuss these solutions further in the subsequent sections of this paper.

Before proceeding to a discussion of the method of calculating the bulk stress in a dilute suspension of spheroidal particles, we remark that the solutions of (3) and (4) which we shall obtain for simple shear flow can be simply extended to many two-dimensional flows. The importance of this extension in enabling our resultant rheological expressions to be applied to a wide variety of bulk flows is obvious. The generalization is based on the fact that, for a suitable choice of axes, any two dimensional flow may be expressed in the form

$$u = (E + \Omega) y, \quad v = (E - \Omega) x, \quad w = 0,$$

with strain rate E and vorticity 2Ω. Referring back to the orbit equations (2), it is clear that the solution of (3) and (4) for simple shear flow also provides the solution for the probability density function for more general two-dimensional flows provided the parameters γ/D and r are replaced by the relative vorticity strength $2\Omega/D$ and an effective aspect ratio r^* given by

$$(r^*)^2 = \frac{(r^2+1)\,\Omega + (r^2-1)\,E}{(r^2+1)\,\Omega - (r^2-1)\,E}.$$

The only limitation on the class of permitted two-dimensional flows arises from the requirement that the particle orbits be closed, the condition for which is

$$(r^*)^2 > 0.$$

Hence, in general, we must require

$$\frac{E}{\Omega} < \frac{r^2+1}{r^2-1}.$$

Although this generalization from simple shear to a wider class of flows has been discussed before (Bretherton 1962; Prager 1957; Chaffey, Takano & Mason 1965) we believe that its significance for suspension rheology has not hitherto been fully appreciated.

(*b*) *The bulk stress tensor for a dilute suspension of spheroids*

It is assumed that the particles are rigid spheroids, the suspending fluid incompressible and Newtonian, and that the suspension concentration is sufficiently small that hydrodynamic interactions among the particles may be neglected. Nevertheless, it is assumed that the necessary length scales exist so that the suspension may be considered, in bulk, as a homogeneous fluid. That is, we assume the existence of a length scale l such that the volume l^3 is large enough to contain a statistically significant number of particles while l is still very small compared to the relevant length scale for the bulk flow field. Finally, the particles are assumed to be *freely* suspended and hence to be free of the action of externally imposed forces or couples. Following Batchelor (1970), we express the bulk (volume-averaged) stress in terms of the volume-averaged velocity and pressure fields as

$$\bar{\sigma}_{ij} = \bar{p}\delta_{ij} + \mu\left(\frac{\partial U_i}{\partial x_j} + \frac{\partial U_j}{\partial x_i}\right) + \sigma'_{ij}, \tag{5}$$

where σ'_{ij} is known as the particle stress and represents the contribution of the suspended particles. The method of calculation of the particle stress is detailed in Batchelor (1970); here we shall only quote the relevant results.

Rotary Brownian motion causes two distinct kinds of effects in the theory of suspension rheology. First of all, the bulk stress is sensitive to the precise distribution of orientations and, as we have already pointed out, this distribution function is affected by the Brownian rotations. In addition, the rotary Brownian motion contributes to the bulk stress in a more direct way by virtue of the effective angular velocity associated with the diffusion process across statistical population gradients in the orientation probability space. This direct contribution was first included by Kirkwood & Auer (1951) and Saito (1951). There still, however, remains some confusion as to the need for its inclusion: Takserman-Krozer & Ziabicki (1963) and Batchelor (1970) omitted or overlooked this term. For the purpose of this paper we have elected to follow Kirkwood and include the direct contribution, although we admit there is not available a conclusive justification for doing so. Brenner (1972) has recently reviewed the problem of the direct contribution.

The direct contribution of the Brownian motions to the bulk stress – in addition to their indirect effect via the probability distribution of the particle orientation – is included by adding an effective particle rotation resulting from the rotary Brownian motion, $-D\nabla(\log N)$, to the hydrodynamically induced rotation for a spheroid undisturbed by Brownian motion effects, $\gamma\mathbf{w}$. These yield a net flux in the orientation space of

$$j = N(\gamma\mathbf{w} - D\nabla(\log N)). \tag{6}$$

The particle stress is linear in the total particle velocity, and hence it is convenient to separate it into two components,

$$\sigma'_{ij} = \sigma^S_{ij} + \sigma^D_{ij}, \tag{7}$$

a strain part σ^S representing the contribution from a spheroid undisturbed by Brownian motion except in so far as it governs the orientation distribution (Batchelor 1970), and an additional part σ^D due to the effective particle rotation caused by the Brownian diffusion.

To obtain the strain part of the particle stress, σ^S, the velocity gradient of the undisturbed flow is first resolved onto the principal axes of the particle at one instantaneous orientation. One can then employ Batchelor's expressions, using Jeffery's hydrodynamic solution to evaluate the required integrals over the particle. The resulting expression for the particle stress must then be resolved back onto the fixed *Oxyz* co-ordinates, and the contribution to the bulk average stress weighted to account for the probability of finding a particle with the particular assumed orientation.

Since the suspension is incompressible, the normal components of the stress are, of course, only determinate within an arbitrary isotropic contribution. Following the common rheological practice we shall eliminate this redundancy by considering only the normal stress differences $\sigma'_{11}-\sigma'_{33}$ and $\sigma'_{22}-\sigma'_{33}$ in the flow and gradient directions, respectively.

Introducing the angle-bracket notation for averages,

$$\langle f(\theta_1,\phi_1)\rangle = \int_0^{\pi} d\theta_1 \int_0^{2\pi} \sin\theta_1\, d\phi_1 f(\theta_1,\phi_1)\, N(\theta_1,\phi_1), \tag{8}$$

the strain contribution to the bulk particle stress is found to be

$$\left.\begin{aligned}
\sigma^S_{11}-\sigma^S_{33} &= \Phi 2\mu E\{-\tfrac{1}{2}A\langle\sin^4\theta_1\sin 4\phi_1\rangle \\
&\qquad + 3A\langle\sin^4\theta_1\sin 2\phi_1\rangle - 2(A-B)\langle\sin^2\theta_1\sin 2\phi_1\rangle\},\\
\sigma^S_{22}-\sigma^S_{33} &= \Phi 2\mu E\{\tfrac{1}{2}A\langle\sin^4\theta_1\sin 4\phi_1\rangle \\
&\qquad + 3A\langle\sin^4\theta_1\sin 2\phi_1\rangle - 2(A-B)\langle\sin^2\theta_1\sin 2\phi_1\rangle\},\\
\sigma^S_{21} &= \sigma^S_{12} = \Phi 2\mu E\{A\langle\sin^4\theta_1\sin^2 2\phi_1\rangle + 2B\langle\sin^2\theta_1\rangle + 2/I_3\},
\end{aligned}\right\} \tag{9}$$

where E is the strain rate $\frac{1}{2}\gamma$, μ is the viscosity of the ambient fluid, Φ the volume concentration of suspended particles and A, B are shape coefficients defined in terms of the ellipsoidal integrals I_i, J_i given in Batchelor (1970):

$$A \equiv \frac{J_3}{I_3 J_1} + \frac{1}{I_3} - \frac{2}{I_1},$$

$$B \equiv \frac{1}{I_1} - \frac{1}{I_3}.$$

We note that the symmetry of the orientation probability about $\theta_1 = \frac{1}{2}\pi$ assures that σ^S_{23} and σ^S_{13} vanish, as expected.

To find σ^D the effective rotation in the orientation space, $-D\nabla(\log N)$, must be converted into an effective angular velocity of the particles. Then again using Jeffery's (1922) solution, the stress for a particular instantaneous orientation is calculated relative to an axis system fixed in the particle, resolved back onto the fixed *Oxyz* axis, and weighted. After one integration by parts to remove

	A	B	$2/I_3$	F
$r \to \infty$	$\dfrac{r^2}{4(\ln 2r - \frac{3}{2})}$	$\dfrac{3\ln 2r - \frac{11}{2}}{r^2}$	2	$\dfrac{3r^2}{(\ln 2r - \frac{1}{2})}$
$r = 1+\epsilon$, $\epsilon \to 0$	$\frac{395}{294}\epsilon^2$	$\frac{15}{28}\epsilon - \frac{895}{1176}\epsilon^2$	$\frac{5}{2}(1 - \frac{2}{7}\epsilon^2 + \frac{1}{3}\epsilon^2)$	9ϵ
$r \to 0$	$\dfrac{5}{3\pi r} + \left(\dfrac{104}{9\pi^2} - 1\right)$	$-\dfrac{4}{3\pi r} + \left(\dfrac{1}{2} - \dfrac{64}{9\pi^2}\right)$	$\dfrac{8}{3\pi r} + O(r)$	$-\dfrac{12}{\pi r} + O(r)$

TABLE 1. The limiting forms of the stress-shape coefficients for spheroids

the differentials of N, the diffusion contribution to the bulk particle stress is found to be

$$\left.\begin{aligned} \sigma_{11}^D - \sigma_{33}^D &= \Phi 2\mu DF\{\tfrac{3}{2}\langle \sin^2\theta_1\rangle - 1 - \tfrac{1}{2}\langle \sin^2\theta_1 \cos 2\phi_1\rangle\}, \\ \sigma_{22}^D - \sigma_{33}^D &= \Phi 2\mu DF\{\tfrac{3}{2}\langle \sin^2\theta_1\rangle - 1 + \tfrac{1}{2}\langle \sin^2\theta_1 \cos 2\phi_1\rangle\}, \\ \sigma_{12}^D = \sigma_{21}^D &= \Phi 2\mu DF\{\tfrac{1}{2}\langle \sin^2\theta_1 \sin 2\phi_1\rangle\}, \end{aligned}\right\} \tag{10}$$

where D is the rotary Brownian diffusion coefficient, and F a shape factor:

$$F \equiv \frac{6(r^2-1)}{r^2 K_3 + K_1}.$$

The integral functions K_3, K_1 were defined in I. Again, symmetry of N with respect to θ_1 causes σ_{23}^D and σ_{13}^D to vanish.

These expressions (9) and (10) for the two parts of the particle stress are essentially the same as those given by Giesekus (1962). The particle contribution to the bulk stress tensor would take the same form for arbitrary axially symmetric particles, as well as the spheroids discussed here, although the four shape functions A, B, F, $2/I_3$ would not be related to the particle aspect ratio in the manner described for spheroids. In addition, it is perhaps worth noting that the average particle stress is symmetric as it should be since no net external couple is acting on the suspension (Batchelor 1970; Leal 1971).

For reference in later sections of the paper, we have tabulated various limiting forms of the shape functions A, B, F and $2/I_3$ in table 1 for spheroids. In subsequent sections we shall use these formulae together with the expressions (9) and (10), and the solutions of equations (3) and (4) to evaluate the bulk stress for various limiting cases of strong and weak Brownian motion, as well as for the case of nearly spherical particles.

3. The orientation distribution function in the limit of very weak rotary Brownian motion

We have indicated in the introduction to this paper that a number of approximate solutions have previously been published for the steady-state orientation distribution function $N(\theta_1, \phi_1)$ represented by the equations (3) and (4). Of these, we call particular attention to the early work of Burgers (1938) and Peterlin (1938), which will be utilized in a subsequent section. These prior solutions were limited either to the case of nearly dominant rotary Brownian motion, $D/\gamma \to \infty$,

or to the case of nearly spherical particles for arbitrary D/γ. The other limiting case of *weak* Brownian rotation ($D/\gamma \to 0$) was considered recently by the present authors (Leal & Hinch 1971). A physical argument was used to obtain the lowest order approximation for the steady-state probability density function N in the limit of high shear rates ($D/\gamma \to 0$), from which it was possible to find the lowest order particle contribution to the effective viscosity μ^* of the suspension, where $\mu^* = \overline{\sigma}_{12}/2E$. In order to calculate the first approximation to the bulk normal stresses and further approximations to the bulk shear stresses in the suspension, the solution for the distribution function must be carried to higher orders of approximation.

In this section, we report the extension of our earlier solution to higher orders via a formal expansion scheme. Before proceeding to these new results, it is worth outlining the main steps of our earlier analysis since their mathematical restatement provides the key to an apparent impasse in the formal expansion procedure.

The essence of our argument in I was that, if rotary Brownian motion were sufficiently weak, a particle would proceed undisturbed around closed Jeffery orbits. The first noticeable effect of the weak Brownian motion would be to yield, after some appropriately long time, an equilibrium distribution for the relative population of the various orbits which does not depend on the initial orientation state of the suspension.

We begin by introducing C, the parameter labelling separate Jeffery orbits, and τ, the phase around these orbits. Fortunately, the orbit period $2\pi\gamma^{-1}(r+r^{-1})$ is the same for all orbits so that the assignment of a single function for the phase around every orbit is trivial. Then, in the *complete absence* of any Brownian motion, the orientation probability density function may be written (I) in the simple form

$$\left.\begin{aligned} N &= f(C)\, g(C,\tau), \\ \text{with} \qquad C &= \tan\theta_1 (r^{-2}\sin^2\phi_1 + \cos^2\phi_1)^{\frac{1}{2}}. \end{aligned}\right\} \tag{11}$$

The function $g(C,\tau)$ represents the orientation distribution around the orbit C and can be evaluated solely from Jeffery's solution to give

$$g(C,\tau) = [r\sin\theta_1\cos^2\theta_1(r^{-2}\sin^2\phi_1 + \cos^2\phi_1)^{\frac{1}{2}}]^{-1}. \tag{12}$$

On the other hand, the function $f(C)$ represents the population distribution of the various orbits. As noted earlier, it would depend on the initial orientation state in the absence of any disturbance effects: the influence of weak Brownian couples renders the distribution determinate, independent of initial conditions. Over a time scale corresponding to several orbit periods the orientation distribution remains relatively unchanged; however, over the (assumed) much longer diffusion time scale a considerable redistribution will occur between different orbits. The equilibrium distribution $f(C)$ is reached when the net diffusional flux across each orbit reaches zero, i.e. when

$$D\oint_{\text{orbit}} \frac{\partial N}{\partial n}\, dl = 0 \tag{13}$$

for each orbit. This integral constraint permits the calculation of $f(C)$. The reader is referred to our earlier paper (I) for the details of that calculation – some

of which is incidently reproduced below – together with a discussion of the results and a comparison with available experimental data.

To obtain higher approximations, we pose a formal expansion in the small parameter D/γ:

$$N = N_0 + \frac{D}{\gamma} N_1 + \left(\frac{D}{\gamma}\right)^2 N_2 + \ldots. \tag{14}$$

Substitution into the equations (3) and (4) yields a zeroth-order problem

$$\nabla . (\mathbf{w} N_0) = 0 \tag{15}$$

together with the higher order problems

$$\nabla . (\mathbf{w} N_{n+1}) = \nabla^2 N_n. \tag{16}$$

These functions N_n are subject to normalization conditions

$$\int_0^{\pi} d\theta_1 \int_0^{2\pi} \sin\theta_1 d\phi_1 N_n = \begin{cases} 1; & n = 0, \\ 0; & n \geqslant 1. \end{cases}$$

We note that, having removed the highest order derivative from the lowest order problem, some non-regular behaviour must be expected in the expansion. For the present time, we choose to ignore this point and proceed to attempt a solution of the regular expansion scheme above. Subsequently, we shall examine the conditions for validity of this solution, and discuss the solution for N in a singular regime.

In order to proceed, a general inversion scheme is required for the advection operator $\nabla . (\mathbf{w}N)$. This can essentially be constructed by transforming from the polar angle co-ordinate system (θ_1, ϕ_1) to the non-orthogonal natural co-ordinates for the orbiting particle (C, τ) using the Jeffery orbit solutions

$$\left.\begin{aligned} \theta_1 &= \tan^{-1}[C(\cos^2\tau + r^2 \sin^2\tau)^{\frac{1}{2}}], \\ \phi_1 &= \tan^{-1}[r \tan\tau]. \end{aligned}\right\} \tag{17}$$

The details of this transformation are discussed in I, where we have also defined the metrics $h(C, \tau)$, $k(C, \tau)$ and the angle $\alpha(C, \tau)$ specifying the skewness of the co-ordinate lines. In this non-orthogonal system the equation (3) becomes

$$\begin{aligned} &\frac{\gamma}{(r + r^{-1}) hk \sin\alpha} \frac{\partial}{\partial\tau}(hk \sin\alpha N) \\ &\quad = \frac{D}{hk \sin\alpha} \left\{ \frac{\partial}{\partial C}\left[\frac{k}{h \sin\alpha} \frac{\partial N}{\partial C} - \cot\alpha \frac{\partial N}{\partial \tau} \right] + \frac{\partial}{\partial \tau}\left[\frac{h}{k \sin\alpha} \frac{\partial N}{\partial \tau} - \cot\alpha \frac{\partial N}{\partial C} \right] \right\}, \end{aligned} \tag{18}$$

where h, k and α are to be regarded as known functions of C and τ. In this co-ordinate system, the inversion of the advection operator reduces to a simple integration, though of course the price paid for this simplicity in the advection term is the added complication in the Laplacian operator.

Employing (18), the problem for the lowest order approximation N_0 is reduced to

$$\frac{\partial}{\partial \tau}(hk \sin\alpha N_0) = 0.$$

The solution is simply
$$N_0 = \frac{f_0(C)}{hk\sin\alpha} \tag{19a}$$

subject to the normalization
$$\int_0^\infty f_0(C)\,dC = \frac{1}{4\pi}. \tag{19b}$$

Hence, our formal expansion procedure has recovered the Jeffery orbit distribution (12), but leaves us with the unknown relative distribution between the various orbits, $f_0(C)$. Mathematically, this indeterminacy is a result of the absence of the highest order derivatives in the governing equation. Physically, the orbit distribution is determined by the Brownian diffusion process, which is not present at this lowest level of approximation.

Leaving $f_0(C)$ temporarily unknown, we proceed to the second approximation N_1. In terms of the (C,τ) co-ordinate system the problem is

$$\frac{\partial}{\partial\tau}(hk\sin\alpha\,N_1) = (r+r^{-1})\left\{\frac{\partial}{\partial C}\left[\frac{k}{h\sin\alpha}\frac{\partial N_0}{\partial C} - \cot\alpha\frac{\partial N_0}{\partial\tau}\right] + \frac{\partial}{\partial\tau}\left[\frac{h}{k\sin\alpha}\frac{\partial N_0}{\partial\tau} - \cot\alpha\frac{\partial N_0}{\partial C}\right]\right\}. \tag{20}$$

The equation (20) can again be integrated with respect to τ hence yielding an expression for N_1 determinate up to another arbitrary orbit distribution function $f_1(C)$: the solution of the homogeneous equation. Clearly, as they stand, the equations at each order of approximation are not sufficient to determine the unknown distribution over the possible orbits. A closure at each level follows, however, from the observation that τ is a periodic variable so that for N_1

$$N_1(C,\tau) = N_1(C,\tau+2\pi).$$

The integration of equation (20) over τ from 0 to 2π thus leads to the integral condition on N_0
$$\frac{d}{dC}\left[\int_0^{2\pi}\left(\frac{k}{h\sin\alpha}\frac{\partial}{\partial C} - \cot\alpha\frac{\partial}{\partial\tau}\right)N_0\,d\tau\right] = 0. \tag{21}$$

The physical implication of this condition is simply that to the order of approximation represented by N_0, the diffusional flux across particle orbits must be constant in the steady state. The more restrictive statement that this constant flux must, in fact, be zero follows by integrating (21) with respect to C and using the symmetry of the distribution about $C = \infty$ ($\theta_1 = \frac{1}{2}\pi$),
$$\int_0^{2\pi}\left(\frac{k}{h\sin\alpha}\frac{\partial}{\partial C} - \cot\alpha\frac{\partial}{\partial\tau}\right)N_0\,d\tau = 0. \tag{22}$$

This is precisely the condition (13) and allows a calculation of $f_0(C)$. In order to conserve space, we refer readers to our earlier paper for the details of this calculation and merely note the solution
$$f_0(C) = \text{const.}\,C(HC^4 + KC^2 + M)\,F^{-\frac{3}{2}}, \tag{23}$$

where
$$F = \left[\frac{2HC^2 + K - (K^2 - 4HM)^{\frac{1}{2}}}{2HC^2 + K + (K^2 - 4HM)^{\frac{1}{2}}}\right]^{(4-K)/(K^2-4HM)^{\frac{1}{2}}}; \quad K^2 > 4HM,$$

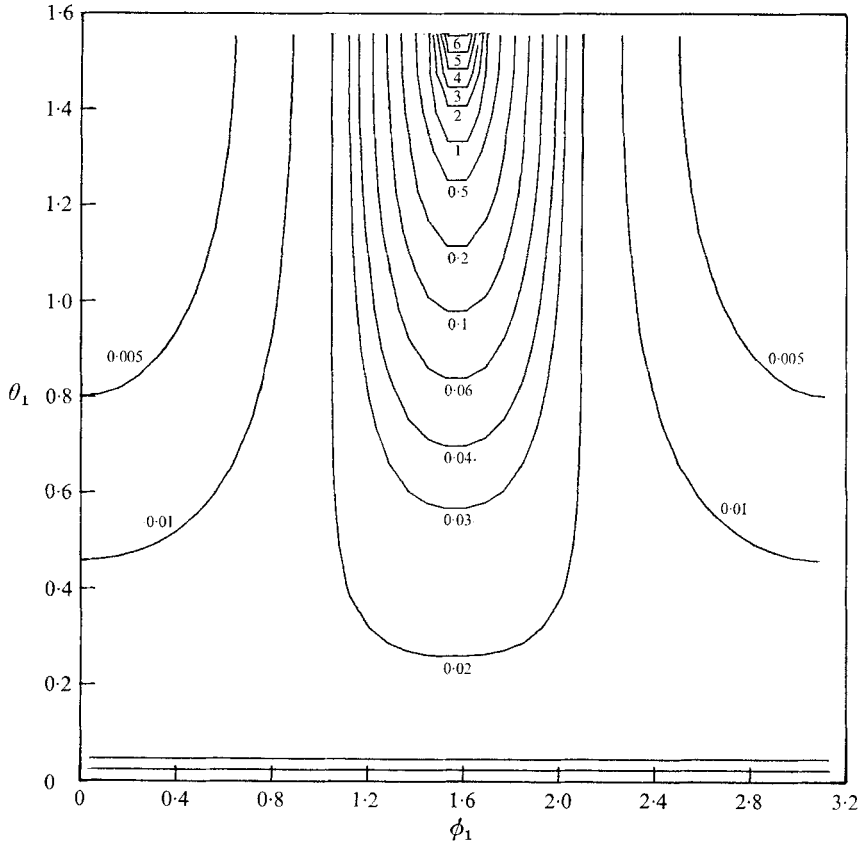

FIGURE 2. Contours of N_0 for $r = 16$.

plus the obvious analytic continuation of F into $K^2 \leqslant 4HM$. The parameters H, K, and M are defined as

$$H(r) = r^2+1; \quad K(r) = \frac{r^2}{4}+\frac{7}{2}+\frac{1}{4r^2}; \quad M(r) = \frac{r^2+1}{r^2}.$$

The constant of integration in (23) is found from the normalization condition (19*b*). An indication of the general form of the distribution function N_0 is contained in the contour plot of N_0 for $r = 16$ shown in figure 2. Particularly noteworthy is the strong population peak for particles nearly aligned with the flow,

$$\theta_1 = \phi_1 = \tfrac{1}{2}\pi.$$

The explanation for this peak is that for large r nearly all of the possible Jeffery orbits (those for $C \gg r^{-1}$ where $|\frac{1}{2}\pi - \phi_3| \gg r^{-1}$ when $\theta_3 = \frac{1}{2}\pi$† – see I) have the majority of the orbit period occurring with $|\theta_3| \lesssim r^{-1}$. The implications of this peaked distribution with regard to the validity of the *regular* perturbation expansion will be discussed in the next section.

Having determined N_0, the calculation of N_1 proceeds as follows. We note, first of all, that the non-homogeneous part of (20) is an even function of τ. Thus, if

† The angles θ_3 and ϕ_3 are defined in figure 1.

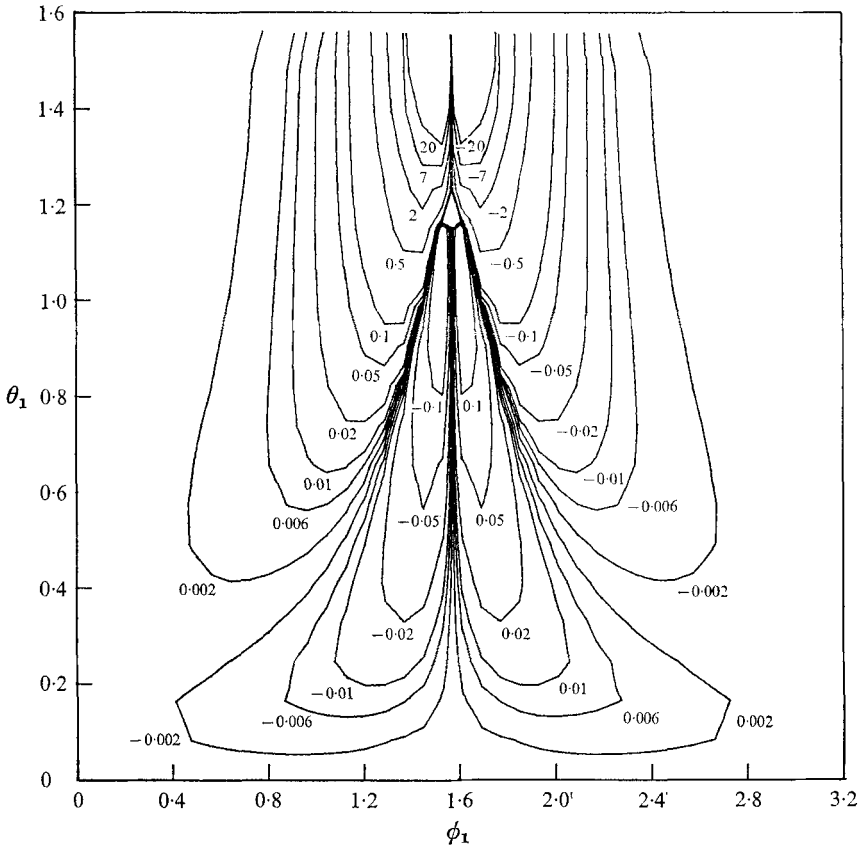

FIGURE 3. Contours of N_1 for $r = 16$.

the τ integration for N_1 is carried out from $\tau = 0$ to some arbitrary value ($\leqslant 2\pi$), the resulting expression for N_1 will be an odd function of τ. Hence, both the normalization condition (20) and the integral constraint on N_1, corresponding to (21) which arises at the next order of approximation, will be satisfied if and only if the homogeneous solution $f_1(C)$ vanishes identically. It may be shown that

$$N_1 hk \sin\alpha = \frac{d^2 f_0}{dC^2}\left[-\frac{r^2-1}{4}(\sin 2\tau)\,C^4 - \frac{(r^2-1)^2}{32r^2}(\sin 4\tau)\,C^2 + \frac{r^2-1}{4r^2}\sin 2\tau\right]$$
$$+\frac{1}{C}\frac{df_0}{dC}\left[-\frac{3(r^2-1)}{2}(\sin 2\tau)\,C^4 + \left(\frac{3}{32}\frac{(r^2-1)^2}{r^2}\sin 4\tau - \frac{r^4-1}{4r^2}\sin 2\tau\right)C^2\right.$$
$$\left.-\frac{3(r^2-1)}{4r^2}\sin 2\tau\right] + \frac{f_0}{C^2}\left[-\frac{3(r^2-1)}{2}(\sin 2\tau)\,C^4\right.$$
$$\left.+\left(-\frac{3}{32}\frac{(r^2-1)^2}{r^2}\sin 4\tau + \frac{r^4-1}{4r^2}\sin 2\tau\right)C^2 + \frac{3(r^2-1)}{4r^2}\sin 2\tau\right]. \quad (24)$$

We illustrate contours of the distribution function N_1 for $r = 16$ in figure 3. The main contribution to N_1 is clearly near the aligned orientation where N_0 was sharply peaked, and corresponds to a shift of the overall distribution

$$N \sim (N_0 + N_1 D/\gamma)$$

toward a position of smaller τ just prior to complete alignment. The main accumulation and deficit near the aligned position are simply understood in terms of a balance between diffusion away from that position which, to first order, occurs with equal probability in either the pre-aligned or post-alignment direction and the advection effect, which acts with unit probability in the single direction of undisturbed rotation about a Jeffery orbit. The two weaker regions of accumulation and deficit at smaller values of θ_1 are a result of cross-orbit diffusion away from the aligned state.

For arbitrary values of the particle aspect ratio r, the normalization of $f_0(C)$ cannot be achieved analytically and so no further simplification of the expression for N_1 is possible. The limiting cases where $r \gg 1, r \ll 1, r-1 = \epsilon$, corresponding approximately to rods, disks and near-spheres, however, allow reduction of the preceding formulae to simpler forms. The main interest of the near-spheres is that they permit a check of our analysis against the results of Sadron (1953), who obtained analytic expressions for N in this case for arbitrary values of D/γ. Since we shall discuss the general near-sphere case in a subsequent section, there is no need to reproduce here the results for the limited subcase $D/\gamma \to 0$. For rod-like particles, we have shown in I that

$$f_0(C) \sim \frac{1}{\pi} \frac{C}{(4C^2+1)^{\frac{3}{2}}} \quad (r \to \infty)$$

so that, following a little algebra, the limiting form for N to $O(D/\gamma)$ is found to be

$$N \sim \frac{1}{hk \sin\alpha} \frac{1}{\pi} \frac{C}{(4C^2+1)^{\frac{3}{2}}} \left\{1 + \frac{Dr^3}{\gamma} \frac{15 \sin 2\tau (1-\cos 2\tau) C^4}{(4C^2+1)^2} + O\left(\frac{Dr^3}{\gamma}\right)^2\right\}. \quad (25)$$

This shows that the correct measure of weak diffusion for $r \gg 1$ is $Dr^3/\gamma \ll 1$ instead of $D/\gamma \ll 1$ as implied in (14). A simple physical argument, essentially requiring the minimum value of the local Péclet number for orientation space advective-diffusion to be large, led the authors to speculate precisely this result in their earlier paper. We shall return to this matter in the next section. In terms of original (θ_1, ϕ_1) variables the expression (25) becomes

$$N(\theta_1, \phi_1) \sim \frac{1}{\pi r} [4 \sin^2\theta_1 (\cos^2\phi_1 + r^{-2}) + \cos^2\theta_1]^{-\frac{3}{2}} \left[1 + \frac{Dr^3}{\gamma} \frac{15 \sin 2\phi_1}{r} \frac{(1 + r^{-4} - \cos^4\phi_1) \sin^4\theta_1 (\cos^2\phi_1 + r^{-2})^3}{\{4 \sin^2\theta_1 (\cos^2\phi_1 + r^{-2}) + \cos^2\theta_1\}^2} + \ldots\right]. \quad (26)$$

In the case of disk-like spheroids ($r \ll 1$),

$$f(C) \sim \frac{1}{\pi} \frac{Cr^2}{(4C^2r^2+1)^{\frac{3}{2}}} \quad (r \to 0),$$

and the first two approximations to N in D/γ give

$$N \sim \frac{1}{hk \sin\alpha} \cdot \frac{1}{\pi} \frac{Cr^2}{(4C^2r^2+1)^{\frac{3}{2}}} \left\{1 - \frac{D}{\gamma r^3} 15 \sin 2\tau (1 + \cos 2\tau) \frac{C^4 r^4}{(4C^2r^2+1)^2} + \ldots\right\}. \quad (27)$$

Similarly to the case $r \to \infty$, the appropriate measure of weak diffusion for $r \ll 1$ is $D/\gamma r^3 \ll 1$.

4. The orientation distribution function in an intermediate regime of weak Brownian motion $D/\gamma \ll 1$, $(\gamma/D)^{\frac{1}{3}} \ll r + r^{-1}$

In the previous section we considered an approximate solution for the orientation distribution which was based on a *regular* perturbation expansion in the small parameter D/γ. A significant characteristic of this solution is that the distribution becomes very sharply peaked in the vicinity of $\theta_1 \sim \phi_1 \sim \frac{1}{2}\pi$ for large values of the aspect ratio, $r \gg 1$. This reflects the fact that the particles spend most of an undisturbed Jeffery orbit nearly aligned with the flow. Similarly, the distribution for $r \ll 1$ becomes sharply peaked near $\theta_1 \sim \frac{1}{2}\pi$, $\phi_1 \sim 0$. Intuitively, it seems possible that, in these extreme cases, rotary Brownian diffusion effects could be negligible at nearly all orientations provided $D/\gamma \ll 1$, but nevertheless be of comparable magnitude with the advection effects in a small region of orientation space near the alignment direction. Confining our attention momentarily to the case of rods, we note that the particles spend nearly all of their total orbit period $2\pi r/\gamma$ within a small angle† $\theta_3 \lesssim r^{-1}$ of full alignment with the flow. For the effects of diffusion to remain small in this region of large gradients in orientation probability requires that the appropriate local Péclet number Dr^3/γ be small as stated in the preceding section. The violation of this condition when D/γ is small requires a singular perturbation expansion for the distribution function. In this section, we consider the case $D/\gamma \ll 1$, but $\gamma/D \ll r^3$. The condition $D/\gamma \ll 1$ ensures that diffussion is negligible nearly everywhere, while $\gamma/D \ll r^3$ (or $(\gamma/D) \ll r^{-3}$ for disks) implies that diffusion is, nevertheless, as important as advection near the special orientation of particle alignment.

For simplicity we shall only consider the derivation of the probability density function for the extreme form of rod-like spheroids. The disk-limit ($r \ll 1$) is entirely identical provided ϕ_1 is rotated by $\frac{1}{2}\pi$. We begin by changing from the (θ_1, ϕ_1) polar co-ordinates to the (θ_3, ϕ_3) co-ordinates which are centred on the alignment direction $\theta_1 = \phi_1 = \frac{1}{2}\pi$. These angles are illustrated in figure 1. The rotation of a spheroid about undisturbed Jeffery orbits is then described by

$$\left.\begin{aligned} \dot{\theta}_3 &= -\frac{\gamma}{r^2+1}(r^2 \sin^2\theta_3 + \cos^2\theta_3)\sin\phi_3, \\ \dot{\phi}_3 &= -\frac{\gamma}{r^2+1}(\cot\theta_3 \cos\phi_3). \end{aligned}\right\} \tag{28}$$

Now as Burgers (1938) also observed, these equations are considerably simplified for slender rods, $r \gg 1$, becoming

$$\dot{\theta}_3 \sim -\gamma \sin^2\theta_3 \sin\phi_3, \quad \dot{\phi}_3 \sim 0, \tag{29}$$

provided only that $\sin\theta_3 \gtrsim r^{-1}$, i.e. the particle orbits reduce to $\phi_3 =$ constant, except for a very small region near the aligned direction.

Now consider the singular region at $\theta_3 \sim 0$. In this region, it is assumed that the effects of advection and diffusion are of equal importance, hence that the local Péclet number is of $O(1)$. Suppose we denote the length scale appropriate to this region $\Delta\theta_3 = \delta$. Then it follows from (29) that the corresponding velocity scale

† See figure 1.

should be $\gamma\delta^2$, and so for the local Péclet number $\gamma\delta^3/D$ to be of order 1 we require

$$\delta = O\left(\frac{D}{\gamma}\right)^{\frac{1}{3}}.$$

The condition $Dr^3/\gamma \gg 1$ is clearly equivalent to the statement that the $(D/\gamma)^{\frac{1}{3}}$ singular region is of much greater extent than the $O(r^{-1})$ subregion in which the rotation differs significantly from (29). As a first approximation, the rotation represented by (29) therefore may be assumed valid in both the outer advection and inner advection–diffusion regions. The smaller region of $O(r^{-1})$ is diffusion dominated and, as is customary for *physical* space boundary-layer problems, it can be neglected at the first-order approximation.

To derive the appropriate governing problem in the inner region, we introduce the stretched variable

$$\rho = (\gamma/D)^{\frac{1}{3}}\theta_3 \tag{30}$$

and the distribution function properly scaled to be consistent with the concentration of the probability at the two singular regions $\theta_3 = 0$ and $\theta_3 = \pi$, or

$$N(\theta_3, \phi_3) \sim (\gamma/D)^{\frac{2}{3}} M(\rho, \phi_3). \tag{31}$$

The governing advection–diffusion equation for M is simply derived using (29), (30), (31) and (3):

$$\frac{1}{\rho}\frac{\partial}{\partial\rho}(\rho^3 \sin\phi_3 M) + \frac{1}{\rho}\frac{\partial}{\partial\rho}\left(\rho\frac{\partial M}{\partial\rho}\right) + \frac{1}{\rho^2}\frac{\partial^2 M}{\partial\phi_3^2} = 0, \tag{32}$$

and the normalization condition (4) becomes

$$\int_0^\infty d\rho \int_0^{2\pi} \rho\, d\phi_3 M = \tfrac{1}{2}. \tag{33}$$

The scaling (30), (31) and the governing equation (32) were actually discovered by Burgers (1938), with the difference that our condition $Dr^3/\gamma \gg 1$ causes his coefficient P to vanish. In spite of the simplification inherent in these equations, Burgers was unable to obtain a satisfactory solution, partly because he failed to appreciate the nature of the interaction between solutions in the inner and outer regions as specified by the matching conditions. In particular, as $\rho \to \infty$ and one enters the overlap region, the advection term in (32) must dominate, giving

$$M(\rho, \phi_3) \to \rho^{-3} g(\phi_3) \quad \text{as} \quad \rho \to \infty, \tag{34}$$

in which $g(\phi_3)$ is an unknown function. Recast in terms of the outer variables, we have

$$N(\theta_3, \phi_3) \to \left(\frac{D}{\gamma}\right)^{\frac{1}{3}} \frac{g(\phi_3)}{\theta_3^3} \quad \text{as} \quad \theta_3 \to 0. \tag{35}$$

In the outer region (which comprises all of the orientation space outside the regions where $\sin\theta_3 \lesssim (D/\gamma)^{\frac{1}{3}}$) advection dominates and the equation (3) becomes

$$-\frac{1}{\sin\theta_3}\frac{\partial}{\partial\theta_3}(\gamma \sin^3\theta_3 \sin\phi_3 N) \sim 0. \tag{36}$$

The outer solution subject to (35) is therefore

$$N(\theta_3, \phi_3) \sim \left(\frac{D}{\gamma}\right)^{\frac{1}{3}} \frac{g(\phi_3)}{\sin^3\theta_3}. \tag{37}$$

This outer solution imposes the final conditions on the inner equation, for since the singular region at $\theta_3 \sim 0$ is mirror-imaged at $\theta_3 \sim \pi$, it follows that

$$g(\phi_3) = g(-\phi_3) = g(\pi - \phi_3). \tag{38}$$

The problem for the first approximation to the orientation distribution function in this intermediate, weak Brownian diffusion regime has been reduced to the solution of (32) subject to the normalization (33) and the matching condition (34), in which the unknown function $g(\phi_3)$ possess the symmetries (38).

We have outlined a scheme for obtaining the first approximation to N in this intermediate regime. Higher order corrections arise from several sources in addition to the obvious one of systematically extending the matched asymptotic solution to include the neglected terms in the basic equations for each region. First, normalization applied to the *uniformly* valid *composite* expansion over the whole orientation space contributes a correction of $O(D/\gamma)$. The neglected deviation of the velocity field from the assumed form (29) in the $O(r^{-1})$ subregion would produce an additional correction of $O(r^{-1}\gamma^{\frac{1}{3}}/D^{\frac{1}{3}})$. Finally, at higher orders of approximation, it is also necessary to consider a strip $|\sin\phi_3| \leqslant O(r^{-1})$ from which orbits do not enter into the singular region.

The solution of (32) subject to (33), (34) and (38) for the unknown functions M and g cannot be obtained by analytical means. Hence, two numerical methods have been utilized. Since these represent standard techniques, whose details are unessential to our discussion, we will only sketch their application to the present problem.

First, a straightforward finite-difference scheme was used, which would have been conceptually uninteresting except for the problem of transforming the matching condition for large ρ into a boundary condition suitable for numerical computation. The difficulty, of course, lies in the fact that the ϕ_3 dependence inherent in $g(\phi_3)$ is *a priori* unknown and must somehow be obtained as part of the solution, apparently producing a hopelessly circular calculation. One apparent '*solution*' would be simply to put the computational outer boundary ρ_∞ at sufficiently large values so that $g(\phi_3)/\rho_\infty^3 \sim 0$ in the numerical sense, thence calculating the field $M(\rho, \phi_3)$ with zeros as the outer boundary condition. This procedure is unsatisfactory for several reasons. First, it effectively ignores the interaction between the inner and outer solutions and hence violates the very spirit of the singular perturbation procedure. Second, it is numerically impractical since the instabilities inherent in the rapidly increasing advection velocities at large ρ severely limit the maximum ρ_∞ allowable for reasonable computational properties. In addition, the function $g(\phi_3)$ which is critical to the bulk stress calculation is left undetermined. These difficulties were minimized by relating the matching condition, and hence $g(\phi_3)$, to an overall integral property of the solution M. This relationship is simply derived by integrating equation (32) once with respect to ρ from $\rho = 0$ to $\rho = \rho_\infty$, using the asymptotic representation $M = g(\phi)/\rho_\infty^3$ to evaluate the integrated expressions at the outer boundary. This allows $g(\phi_3)$ to be calculated from an assumed solution for M. An obvious iterative process is thus possible. One iteration consists of the calculation of a convergent solution for M using an assumed functional form for $g(\phi_3)$ to supply

boundary conditions at ρ_∞, followed by a re-calculation of $g(\phi_3)$ from this new solution for M. In principle this procedure could be used to generate solutions of high accuracy provided the whole scheme converges. The solutions which we actually calculated were of only limited accuracy for two reasons. First, and most important, the necessary computation time was found to be excessive so that our calculations were terminated after only two complete iterations. Second, the co-ordinate singularity at $\rho = 0$ was rather poorly resolved by our finite-difference scheme. In view of the rather modest convergence after our two iterations we felt further refinements in the treatment at the origin to be unwarranted. The initial input for these calculations consisted of $g(\phi_3) = 0$ with the outer boundary located at $\rho_\infty = 11$.

Because of the necessity of terminating the calculations after only two complete iterations and the difficulties in dealing with the co-ordinate singularity, we considered it necessary to check the results using a Galerkin scheme. This alternative approach also suffered from certain deficiencies. First there was no obvious set of complete orthogonal polynomials for the radial direction which fitted into the matching condition. Second, it was found that the usual method of Galerkin, being equivalent to reducing the mean-square error in satisfying the equation, did not place sufficient emphasis on the solution for large ρ to prevent the Laplacian term from dominating, which then caused a constant to be selected as the solution. This difficulty was overcome by minimizing the mean-square *fractional* error calculated by dividing the local error by the local value of M. This mean-square fractional error was reduced from a value of 45 using a one term approximation for M to 5 when the number of included functions was increased to 7. The results of these calculations for M are plotted in figure 4. Moderate agreement was found between this and the numerical solution and this could presumably be improved by calculating both of the solutions to higher accuracy.

As in the regular perturbation case, the solution here predicts a population peak very near the aligned position with a slight skewness in favour of the pre-aligned orientations relative to the post-alignment positions. It should be remembered that in spite of the qualitative resemblance of the results in figure 4 with those shown in figures 2 and 3, the peak in the orientation density function is really much stronger for the present intermediate regime since the scale of the entire inner region shown in figure 4 is only $O(D/\gamma)^{\frac{1}{3}}$.

Combining the results of this and the preceding section with the earlier calculations of Burgers' (1938) and of Peterlin (1938), it is possible to calculate the bulk stress for a number of limiting cases. These calculations are reported in the following section.

5. Calculations of the bulk stress

(*a*) *Strong Brownian motions*, $D/\gamma \gg 1$

We have already indicated, in the introduction, that in spite of the heavy study of rotary Brownian motion effect on rheological properties of dilute suspensions of rigid spheroids only Giesekus (1962) has actually considered the full bulk

stress tensor. His calculations were carried out for the limiting case of very strong rotary Brownian motion, and are summarized here before we proceed to similar calculations for the weak Brownian motion problem.

Giesekus (1962) employed an expansion for the distribution function N in terms of the small parameter γ/D to calculate the angle averages in (9) and (10), yielding expressions for the two parts of the article stress σ^S and σ^D which can be written as

$$\left.\begin{aligned}
\sigma_{12}^S &= \Phi\mu\gamma\left\{\tfrac{4}{15}A+\tfrac{4}{3}B+\frac{2}{I_3}+O(\gamma^2/D^2)\right\},\\
\sigma_{11}^S-\sigma_{33}^S &= \Phi\mu\gamma\left\{\frac{\gamma}{D}\cdot\frac{r^2-1}{r^2+1}\frac{6(2A+7B)}{315}+O(\gamma^3/D^3)\right\},\\
\sigma_{22}^S-\sigma_{33}^S &= \Phi\mu\gamma\left\{\frac{\gamma}{D}\cdot\frac{r^1-1}{r^2+1}\cdot\frac{6(2A+7B)}{315}+O(\gamma^3/D^3)\right\},\\
\sigma_{12}^D &= \Phi\mu\gamma\left\{\frac{1}{15}\frac{r^2-1}{r^2+1}.F+O(\gamma^2/D^2)\right\},\\
\sigma_{11}^D-\sigma_{33}^D &= \Phi\mu\gamma\left\{\frac{\gamma}{D}\left[\frac{1}{210}\left(\frac{r^2-1}{r^2+1}\right)^2+\frac{1}{90}\left(\frac{r^2-1}{r^2+1}\right)\right]F+O(\gamma^3/D^3)\right\},\\
\sigma_{22}^D-\sigma_{33}^D &= \Phi\mu\gamma\left\{\frac{\gamma}{D}\left[\frac{1}{210}\left(\frac{r^2-1}{r^2+1}\right)^2-\frac{1}{90}\left(\frac{r^2-1}{r^2+1}\right)\right]F+O(\gamma^3/D^3)\right\}.
\end{aligned}\right\}\tag{39}$$

Several features of interest are inherent in these expressions and should be noted here. These are most conveniently presented by introducing three shape factors $f_0^S(r)$, $f_1^S(r)$ and $f_2^S(r)$, which allow the full particle stress ($\sigma' = \sigma^S+\sigma^D$) to be re-expressed:

$$\left.\begin{aligned}
\sigma'_{12} &= \Phi\mu\gamma\{f_0^S(r)+O(\gamma^2/D^2)\},\\
\sigma'_{11}-\sigma'_{33} &= \Phi\mu\gamma\left\{\frac{\gamma}{D}f_1^S(r)+O(\gamma^3/D^3)\right\},\\
\sigma'_{22}-\sigma'_{33} &= \Phi\mu\gamma\left\{\frac{\gamma}{D}f_2^S(r)+O(\gamma^3/D^3)\right\}.
\end{aligned}\right\}\tag{40}$$

As required, the normal stress differences are even functions of γ. We note that this forces them to be $O(\gamma/D)$ and so an order of magnitude smaller than the additional shear stress. We have followed Giesekus and plotted the shape functions in figures 5 and 6 as a function of r. In addition, we show the limiting forms for rod-like, disk-like and nearly spherical spheroids. The analytic expressions for the shape functions in these limiting cases are given in table 2. Both of the normal stress differences are non-zero provided $r \neq 1$, hence violating the Weissenberg hypothesis. However, the streamwise component is considerably the larger of the two. We finally note that, since the expansion of the distribution function N for small γ/D essentially represents an expansion in small departures from equilibrium, we can recast the formulae (40) into the second-order fluid form

$$\sigma = -pI+\eta_0 A_1-\eta_2 A_2+\alpha_1 A_1^2,$$

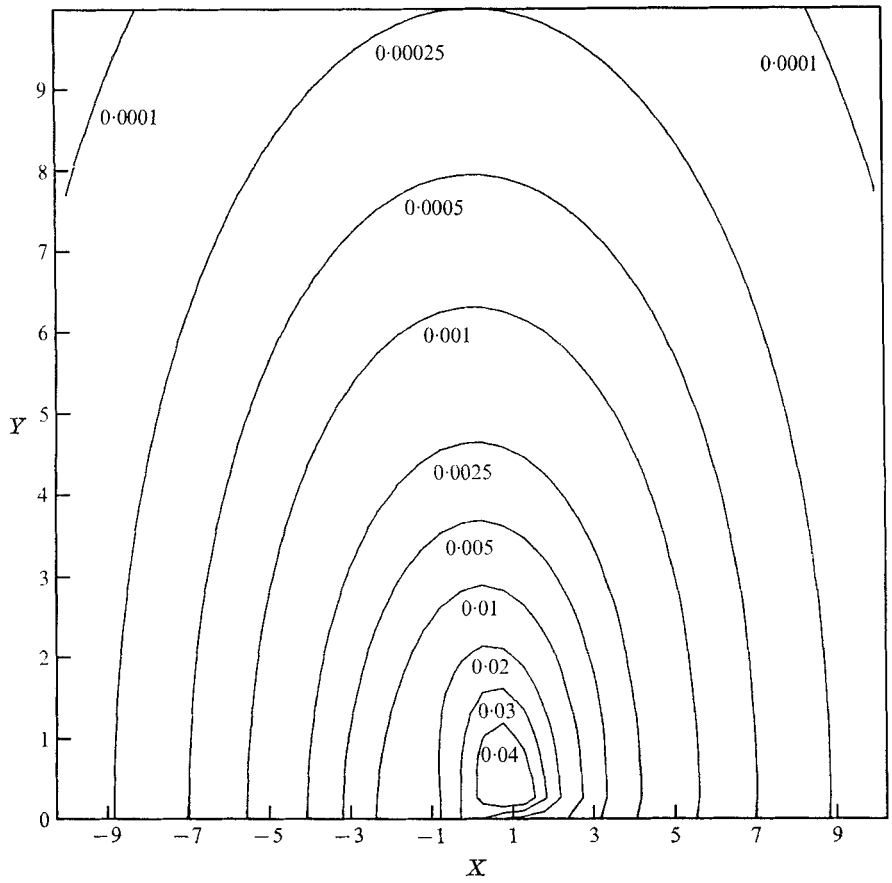

FIGURE 4. Contours of the distribution function M in the boundary-layer co-ordinates. $X = \rho\cos\phi_3$, $Y = \rho\sin\phi_3$.

	$f_0^S(r)$	$f_1^S(r)$	$f_2^S(s)$
$r \to \infty$	$\frac{4}{15}\frac{r^2}{\ln r}$	$\frac{2}{35}\frac{r^2}{\ln r}$	$-\frac{1}{105}\frac{r^2}{\ln r}$
$r = 1+\epsilon$ $\epsilon \to 0$	$\frac{5}{2}+\frac{171}{2205}\epsilon^2$	$\frac{6}{35}\epsilon^2$	$-\frac{1}{35}\epsilon^2$
$r \to 0$	$\frac{32}{15\pi}\frac{1}{r}$	$\frac{4}{21\pi}\frac{1}{r}$	$-\frac{8}{105\pi}\frac{1}{r}$

TABLE 2. The stress-shape factors for strong Brownian motions

in which A_i are the well-known Rivlin–Ericksen tensors. The coefficients for this rotary Brownian motion second-order fluid are

$$\left.\begin{aligned} \eta_0 &= \mu[1+\Phi f_0^S(r)], \\ \eta_2 &= \mu\Phi[f_1^S(r) - f_2^S(r)]/2D, \\ \alpha_1 &= \mu\Phi[f_1^S(s)]/D, \end{aligned}\right\} \tag{41}$$

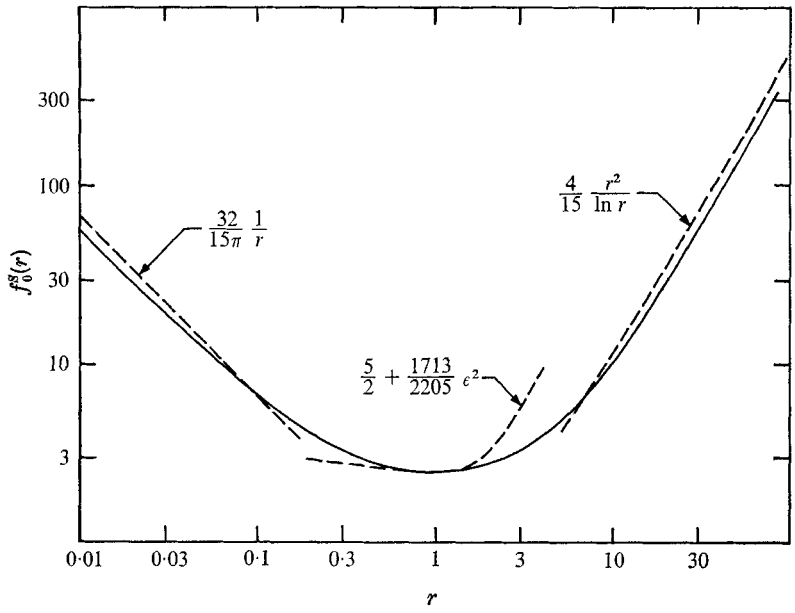

FIGURE 5. The shear-stress function $f_0^S(r)$ as a function of particle aspect ratio.

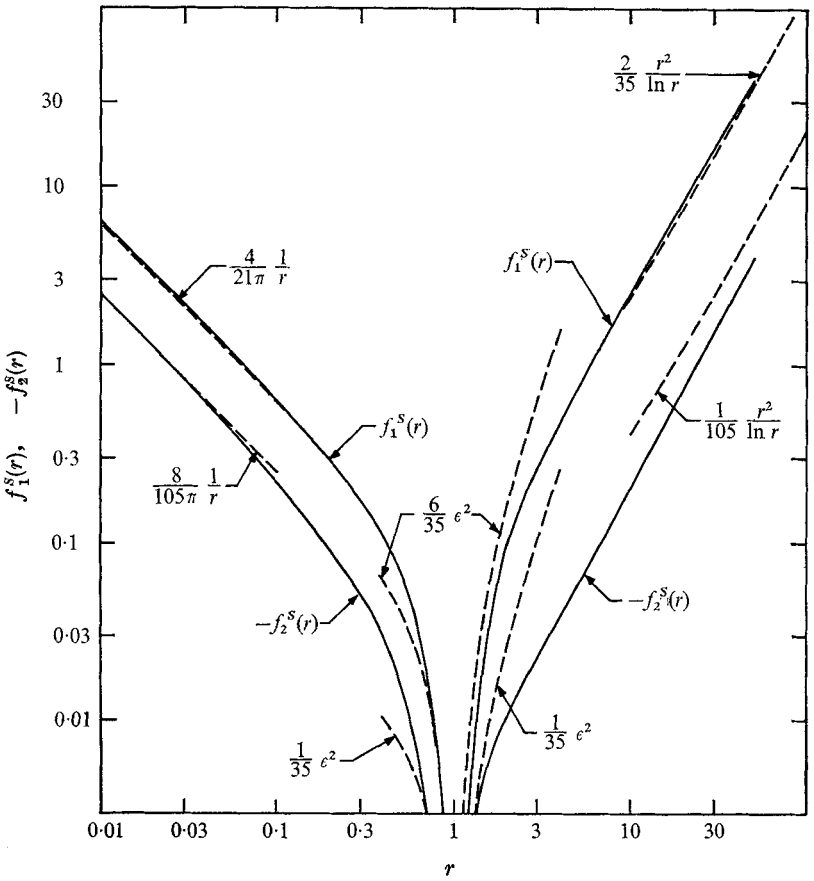

FIGURE 6. The normal-stress functions $f_1^S(r)$ and $f_2^S(r)$ as a function of the particle aspect ratio.

where D^{-1} can be interpreted as the relaxation time for the fluid. A similar identification with the second-order fluid models of continuum mechanics was inherent in the work of Giesekus.

In the subsequent portions of this section, we shall extend the class of suspension parameters where the full rheology is described to include both the cases of weak rotary Brownian motion, and nearly spherical particles for rotary Brownian motion of arbitrary strength. The former are of particular interest since the large departures from orientational equilibrium provide a strong contrast with the near-equilibrium, second-order fluid theory discussed above. Taken together, the cases of strong and weak rotary Brownian motion allow a qualitative description of the rheological behaviour of the suspension over the complete range of shear rates, even with r considerably different from 1. The near-sphere case does not seem to have appeared explicitly in print before, although the orientation distribution function has been known for some time. It is included here mainly because it provides a convenient check on our limiting results, as well as an instructive bridge of the intermediate region of rotary Brownian motion where neither Giesekus's (1962) work nor the weak Brownian motion theories are valid.

(*b*) *Near spheres*, $r \sim 1$

For spheroids whose shape differs little from spherical it is possible to obtain an approximate solution of the orientation distribution function which is valid for all shear rates leading, as indicated previously, to explicit nonlinear constitutive equations which hold from the strong Brownian motion limit considered above to the weak Brownian motion limit to be presented in the next portion of this section. The expression for the distribution function utilized here is originally due to Peterlin (1938), and is based on the qualitative observation that the undisturbed shear flow will only cause small departures from the uniform orientation state so long as the effective measure of the strain rate $E(r^2-1)/(r^2+1)$ is small compared with either the vorticity or the inverse Brownian relaxation time.

To recover Peterlin's solution one formally expands in the small parameter $(r^2-1)/(r^2+1)$:

$$N = N_0 + \left(\frac{r^2-1}{r^2+1}\right) N_1 + \left(\frac{r^2-1}{r^2+1}\right)^2 N_2 + \ldots.$$

The zeroth-order problem is then

$$D\nabla^2 N_0 - \frac{\gamma}{2}\frac{\partial N_0}{\partial \phi_1} = 0.$$

At the lowest order of approximation, the spheroids are spheres. Any axis of a sphere can be a principal axis, so that the orientation of 'the' principal axis must be purely random. Thus with normalization we have

$$N_0 = 1/4\pi.$$

At subsequent orders

$$D\nabla^2 N_{n+1} - \frac{\gamma}{2}\frac{\partial N_{n+1}}{\partial \phi_1} = \gamma\left\{\frac{1}{\sin\theta_1}\frac{\partial}{\partial\theta_1}(\sin^2\theta_1 \cos\theta_1 \sin 2\phi_1 N_n) + \frac{\partial}{\partial\phi_1}(\cos 2\phi_1 N_n)\right\}.$$

To solve this equation, it is most convenient to express the known right-hand side in terms of the eigenfunctions of the left-hand side operator. These eigenfunctions are spherical surface harmonics and the eigenvalues are complex. To the order of $(r^2-1)/(r^2+1)$, the orientation distribution function is simply

$$N = \frac{1}{4\pi}\left[1+\left(\frac{r^2-1}{r^2+1}\right)\frac{3\sin^2\theta_1\sin\{2\phi_1-\tan^{-1}(\gamma/6D)\}}{2[1+(6D/\gamma)^2]^{\frac{1}{2}}}\right]. \tag{42}$$

The angle averages can be calculated to the relevant approximation to yield the two parts of the stress tensor. Writing $r = 1+\epsilon$, these are

$$\left.\begin{aligned}
\sigma_{12}^S &= \Phi\mu\gamma\,[\tfrac{5}{2}+\tfrac{78}{441}\epsilon^2+O(\epsilon^3)],\\
\sigma_{11}^S-\sigma_{33}^S = \sigma_{22}^S-\sigma_{33}^S &= \Phi\mu\gamma\left[\tfrac{3}{7}\epsilon^2\frac{6D/\gamma}{1+(6D/\gamma)^2}+O(\epsilon^3)\right],\\
\sigma_{12}^D &= \Phi\mu\gamma\left[\tfrac{3}{5}\epsilon^2\frac{(6D/\gamma)^2}{1+(6D/\gamma)^2}+O(\epsilon^3)\right],\\
\sigma_{11}^D-\sigma_{33}^D = \sigma_{33}^D-\sigma_{22}^D &= \Phi\mu\gamma\left[\tfrac{3}{5}\epsilon^2\frac{6D/\gamma}{1+(6D/\gamma)^2}+O(\epsilon^3)\right].
\end{aligned}\right\} \tag{43}$$

Hence

$$\left.\begin{aligned}
\sigma'_{12} &= \Phi\mu\gamma\left[\tfrac{5}{2}+\epsilon^2\left(\frac{78}{441}+\frac{3}{5}\left(\frac{(6D/\gamma)^2}{1+(6D/\gamma)^2}\right)\right)+O(\epsilon^3)\right],\\
\sigma'_{11}-\sigma'_{33} &= \Phi\mu\gamma\left[\tfrac{36}{35}\epsilon^2\frac{6D/\gamma}{1+(6D/\gamma)^2}+O(\epsilon)^3\right],\\
\sigma'_{22}-\sigma'_{33} &= \Phi\mu\gamma\left[-\tfrac{6}{35}\epsilon^2\frac{6D/\gamma}{1+(6D/\gamma)^2}+O(\epsilon^3)\right].
\end{aligned}\right\} \tag{44}$$

The shear stress is most conveniently discussed in terms of the effective viscosity μ^*, the shear stress divided by the shear rate,

$$\mu^* = \mu\left[1+\Phi\left\{\tfrac{5}{2}+\epsilon^2\left(\frac{78}{441}+\frac{3}{5}\left(\frac{(6D/\gamma)^2}{1+(6D/\gamma)^2}\right)\right)\right\}+\ldots\right]. \tag{45}$$

We note several interesting features of this expression. First, the effect of particle non-sphericity is very weak, producing only a quadratic, $O(\epsilon^2)$, departure from the value for perfect spheres. Interestingly, although the numerical variation is small, of order $\epsilon^2\Phi$, the dependence of μ^* on γ shows a shear-thinning character, with a zero-shear limiting viscosity $\mu\{1+\Phi(\frac{5}{2}+\frac{1713}{2205}\epsilon^2)\}$ and high shear limiting value of $\mu\{1+\Phi(\frac{5}{2}+\frac{78}{441}\epsilon^2)\}$.

The shear dependence of the normal stress differences is shown in figure 7. As the shear rate increases, the normal stress differences initially rise quadratically from the limiting value of zero for very small shear rates, however, as the shear rate increases further, they both tend to limiting values which are independent of γ. So far as we are aware, this interesting shear-dependent behaviour of the normal stress differences has not been previously noted. A second feature of the normal stress differences is the fact that their ratio $(\sigma_{11}-\sigma_{33})/(\sigma_{33}-\sigma_{22})$ retains a constant value of six, independent of γ. Thus while the Weissenberg

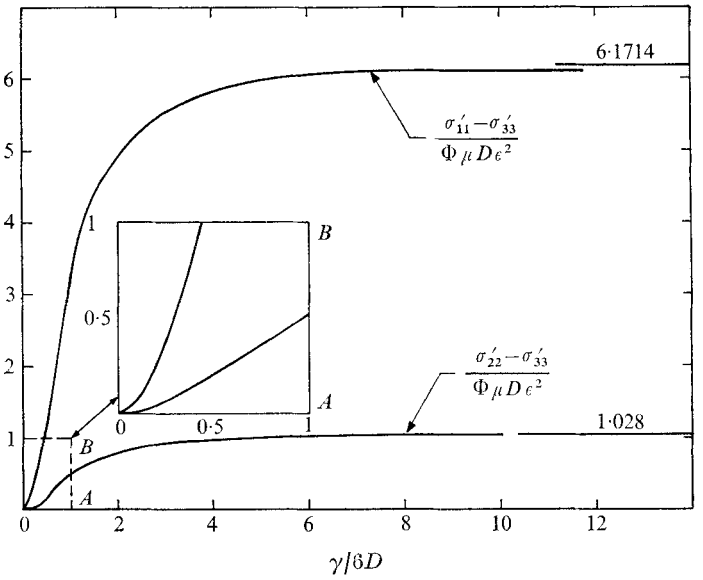

FIGURE 7. The shear dependence of the normal stress differences for a suspension of near-spheres.

hypothesis is not valid, the streamwise normal stress difference nevertheless is found to be considerably larger than the normal stress difference in the velocity gradient direction.

(c) *Weak Brownian motion*, $(r^3+r^{-3})\,D/\gamma \ll 1$

In §3, we obtained an expression, valid to second order, for the steady-state orientation distribution function. For general values of the aspect ratio, the angle averages required in the bulk stress calculation must be evaluated numerically. We have tabulated the results of these computations in table 3. For comparison, we also give values calculated from asymptotic formulae corresponding to the limiting forms of the distribution functions (25) and (27). Examining these results in conjunction with the expressions (9) and (10) for σ^S and σ^D, respectively, we immediately note that N_0 contributes to the shear stress portion of σ^S and to the normal stresses of σ^D, while N_1 contributes only to the normal stress portions of σ^S. It is instructive, once again, to express the results in terms of new shape functions f_0^W, f_1^W and f_2^W.

$$\left.\begin{aligned}\sigma'_{11} &= \Phi\mu\gamma\{f_0^W(r)+O(D^2/\gamma^2)\},\\ \sigma'_{11}-\sigma'_{33} &= \Phi\mu\gamma\{(D/\gamma)f_1^W(r)+O(D^3/\gamma^3)\},\\ \sigma'_{22}-\sigma'_{33} &= \Phi\mu\gamma\{(D/\gamma)f_2^W(r)+O(D^3/\gamma^3)\}.\end{aligned}\right\} \tag{46}$$

These shape functions are plotted in figures 8 and 9. Additionally, corresponding approximate forms for rod-like ($r \gg 1$), near-spherical and disk-like ($r \ll 1$) spheroids, displayed in table 4, have also been included in these figures. Finally, for comparison, we have also shown the numerical results obtained by Scheraga (1955) for $\gamma/D = 60$. Of course, when $\gamma/D = 60$, the condition $\gamma/D \gg (r^3+r^{-3})$ holds at best for $\frac{1}{4} < r < 4$ so that it is impossible to expect agreement between Scheraga (1955) and our own results for the *weak* Brownian motion limit when r

Aspect ratio	1·05	2	3	4	5	7	10	16	25	50	100
$\langle \sin^2\theta_1 \rangle$											
Calculated	0·663	0·690	0·727	0·758	0·784	0·823	0·862	0·905	0·936	0·968	0·986
$1-1\cdot792/r$	−0·705	0·104	0·402	0·522	0·631	0·744	0·821	0·888	0·928	0·964	0·982
$\langle \sin^2\theta_1 \sin 2\phi_1 \rangle$											
Calculated $\times \gamma/D$	0·116	2·16	4·96	8·66	13·3	25·5	51.5	129	313	1245	4996
$\frac{1}{2}r^2$	0·551	2·00	4·5	8·00	12·5	25·5	50·0	128	313	1250	5000
$\langle \sin^2\theta_1 \cos 2\phi_1 \rangle$											
Calculated	−0·0194	−0·272	−0·419	−0·514	−0·581	−0·672	−0·753	−0·837	−0·892	−0·939	−0·958
-1	−1	−1	−1	−1	−1	−1	−1	−1	−1	−1	−1
$\langle \sin^4\theta_1 \sin 2\phi_1 \rangle$											
Calculated $\times \gamma/D$	0·0091	1·90	4·48	8·01	12·5	24·5	49·9	127	310	1243	4995
$\frac{1}{2}r^2$	0·551	2·0	4·5	8·00	12·5	24·5	50·0	128	313	1250	5000
$\langle \sin^4\theta_1 \sin^2 2\phi_1 \rangle$											
Calculated $\times \gamma/D$	0·264	0·238	0·204	0·176	0·155	0·124	0·0961	0·0672	0·0461	0·0208	0·01217
$1\cdot261/r$	1·20	0·630	0·420	0·315	0·253	0·180	0·126	0·0780	0·0504	0·0253	0·0126
$\langle \sin^4\theta_1 \sin 4\phi_1 \rangle$											
Calculated	−0·00721	−1·81	−6·14	−12·7	−21·3	−44·7	−95·0	−250	−616	−2480	−9998
$-r^2$	−1·10	−4·00	−9·00	−16·0	−25·0	−49·0	−100	−256	−625	−2500	−10000

Note: The results for aspect ratios less than unity may be obtained utilizing the transformation $r \to 1/r$, $\theta_1, \to \theta_1$, $\phi_1 \to \phi_1 + \frac{1}{2}\pi$.

TABLE 3. The angle averages for weak Brownian motions. The calculated values were obtained numerically from the distribution (24). The asymptotic values at large aspect ratio are given below, and are found from the limiting distribution (25).

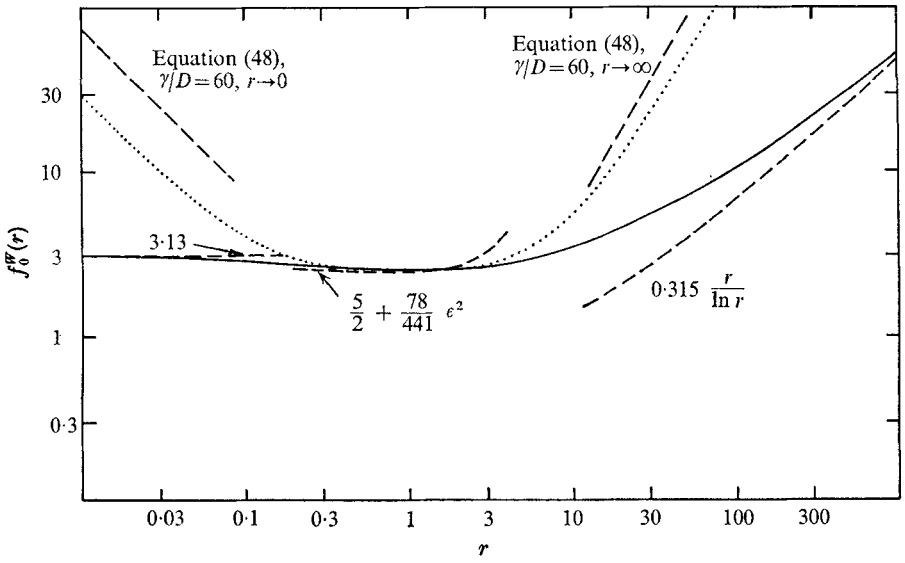

FIGURE 8. The shear-stress f_0^W is shown as a function of particle aspect ratio r by the continuous curve. The dashed curves are asymptotic forms. Schieraga's numerical results at $\gamma/D = 60$ are shown by the dotted curve.

	$f_0^W(r)$	$f_1^W(r)$	$f_2^W(r)$
$r \to \infty$	$0{\cdot}315\frac{r}{\ln r}$	$\frac{1}{4}\frac{r^4}{\ln r}$	$o\left(\frac{r^4}{\ln r}\right)$
$r = 1+\epsilon$ $\epsilon \to 0$	$\frac{5}{2}+\frac{78}{441}\epsilon^2$	$\frac{216}{35}\epsilon^2$	$-\frac{36}{35}\epsilon^2$
$r \to 0$	3.13	$\frac{4}{3\pi}\frac{1}{r^3}$	$-\frac{1}{3\pi}\frac{1}{r^3}$

TABLE 4. The stress-shape factors for weak Brownian motions

is much different from unity. Finally, we note that, for extreme r, the strain part of the stress tensor dominates the diffusion part because the very slow rotations associated with the aligned orientation amplify the gradients of N_0 and hence cause N_1 to be two orders of magnitude in r larger.

Before discussing these results in more detail, it is useful to consider the nature of the bulk stress in the intermediate range.

(*d*) *The intermediate regime,* $D/\gamma \ll 1, (\gamma/D)^{\frac{1}{3}} \ll r + r^{-1}$

We have considered, in § 4, the solution for the steady-state orientation distribution function in the intermediate regime where $D/\gamma \ll 1$ but the particle aspect ratio is extreme. Three integrals of the solution are required for the angle averages to be used in the bulk stress tensor. The numerical values calculated from our

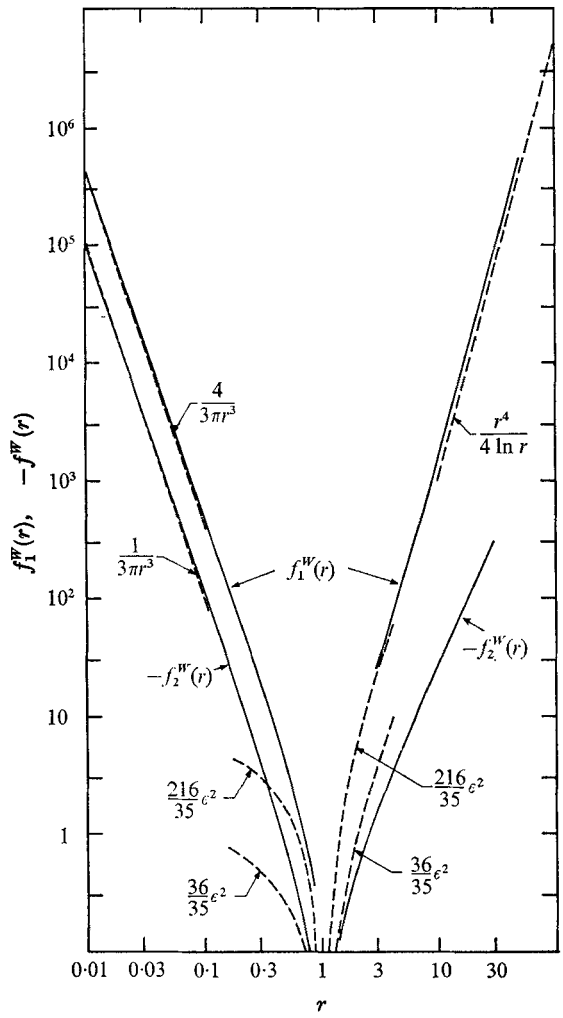

FIGURE 9. The normal stress functions $f_1^W(r)$ and $f_2^W(r)$ as a function of particle aspect ratio.

approximate solutions for rods are

$$I_1^N = \int_0^\infty d\rho \int_0^{2\pi} \rho d\phi_3 \rho \sin\phi_3 M = 0{\cdot}09,$$

$$I_2^N = \int_0^{2\pi} d\phi_3 \cos^2\phi_3 g(\phi_3) = 0{\cdot}6,$$

$$I_3^N = \int_0^{2\pi} d\phi_3 \sin^2\phi_3 g(\phi_3) = 0{\cdot}3.$$

The angle averages obtained from the matched asymptotic expansion (31) and (35) are hence

$$\left.\begin{aligned} \langle\sin^2\theta_1\rangle \sim 1, \quad \langle\sin^2\theta_1\cos 2\phi_1\rangle \sim -1, \\ \langle\cos^2\theta_1\rangle \sim (D/\gamma)^{\frac{1}{3}}\pi I_2^N = 2(D/\gamma)^{\frac{1}{3}}, \\ \langle\sin^4\theta_1\sin^2 2\phi_1\rangle \sim (D/\gamma)^{\frac{1}{3}}\, 2\pi I_3^N = 2(D/\gamma)^{\frac{1}{3}}, \\ -\tfrac{1}{2}\langle\sin^4\theta_1\sin 4\phi_1\rangle \sim \langle\sin^4\theta_1\sin 2\phi_1\rangle \sim \langle\sin^2\theta_1\sin 2\phi_1\rangle \\ \sim (D/\gamma)^{\frac{1}{3}} 4 I_1^N = 0{\cdot}4\,(D/\gamma)^{\frac{1}{3}}. \end{aligned}\right\} \tag{47}$$

The results for disks are obtained by replacing ϕ_1 by $\phi_1 + \frac{1}{2}\pi$. In the calculation of the bulk particle stress, the direct Brownian diffusion contribution is negligible because the small rotation rates amplify the gradients by order $(\gamma/D)^{\frac{2}{3}}$. The limiting forms for the bulk particle stress are

$$\sigma'_{12} \sim \Phi\mu\gamma \left|\frac{D}{\gamma}\right|^{\frac{1}{3}} \begin{cases} 0{\cdot}5\, r^2/\ln r & (r \to \infty), \\ 3/r & (r \to 0), \end{cases} \tag{48a}$$

$$\sigma'_{11} - \sigma'_{33} \sim \Phi\mu\gamma \left(\frac{D}{\gamma}\right)^{\frac{1}{3}} \begin{cases} 0{\cdot}2\, r^2/\ln r & (r \to \infty), \\ 0{\cdot}3/r & (r \to 0), \end{cases} \tag{48b}$$

$$\sigma'_{22} - \sigma'_{33} \sim \Phi\mu\gamma \left(\frac{D}{\gamma}\right)^{\frac{1}{3}} \begin{cases} o(1)\, r^2/\ln r & (r \to \infty), \\ -0{\cdot}08/r & (r \to 0). \end{cases} \tag{48c}$$

Combining these various limiting expressions for the bulk stress, it is possible to piece together a qualitative picture of the rheological behaviour of the suspension for arbitrary shear rates γ and aspect ratio r. This is discussed in the following section.

6. Conclusions

In the previous section, we have derived expressions for the bulk stress for various limiting cases of particle shape and shear strength. When the particles are nearly spherical, it was shown that the suspension exhibits shear-thinning with constant limiting values of the effective viscosity for very large and very small γ/D, and in addition, that the normal stresses would increase quadratically with γ for small γ/D, eventually approaching a value dependent on D only for γ/D sufficiently large. Although this behaviour is interesting, the departures from equilibrium are small, so the results differ very little, numerically, from those for spherical particles.

While a continuous description of stress variation with strain rate is not possible for the general case where r is not near to unity, we can achieve a qualitative feeling for the variation of the stress components by piecing together the limiting cases of very strong, very weak and intermediate strength rotary Brownian motion. First of all, Giesekus (1962) showed that for sufficiently small values of γ/D the shear stress increases linearly with γ, corresponding to a constant low-shear effective viscosity, while the normal stresses are an order of magnitude smaller than the extra shear and increase as γ^2. The streamwise normal stress difference is consistently larger than the transverse difference.

On the other hand, when γ is so large that the weak Brownian motion approximation is valid, $r^3 + r^{-3} \ll \gamma/D$, the shear stress is again a linear function γ. The corresponding limiting value of the effective viscosity is, by inspection of tables 2 and 4, smaller for all r than that for the strong Brownian motion limit of Giesekus (1962). Moreover, for extreme aspect ratios this shear thinning represents a *large* change (by a factor r) in the additional effective viscosity. This reflects the high degree of particle alignment with the flow at large shear rates together with the fact that the disruption of the basic shear flow is minimized for such an orientation. Note that a similar alignment process for weak Brownian couples in axisymmetric flow causes strain thickening (Takserman-Krozer & Ziabicki 1963).

Even more interesting is the fact, obvious from (46), that the normal stress for sufficiently large γ/D are found to be constant independent of the shear rate and considerably larger than those calculated in the strong Brownian motion case. The normal stresses are again found to be an order of magnitude in $(r^3+r^{-3})\,D/\gamma$ smaller than the particle contributions to the shear stress, essentially a result of the fact that the normal stresses must be even functions of the shear rate. Even without the results in the intermediate regime, it is now clear that the suspension for general r behaves very much like that for $r \sim 1$, with the exception that the magnitude of shear thinning and of the normal stress increase are both greatly enhanced.

Last, a portion of the transition region between the high and low shear limiting results is illustrated by our intermediate regime. Here, the intrinsic effective viscosity decreases with increasing shear strength as $(D/\gamma)^{\frac{1}{3}}$ while the normal stress components increase like $(\gamma/D)^{\frac{2}{3}}$. Particularly surprising in view of the two limiting cases is the comparable magnitude of the particle-induced shear and normal stresses. In addition, we note that the second (transverse) normal stress difference vanishes for rods to the order considered in this regime. To compare our results in this intermediate regime with the numerical calculations of Scheraga (1955), we have plotted in figure 8 the particle-induced shear stress at $\gamma/D = 60$ calculated from equation (48) for the limiting cases $r \to \infty$ and $r \to 0$. It is not obvious whether the apparent discrepancies should be ascribed to inaccuracies in the calculated angle averages (47), or whether the numerical convergence of Peterlin's power series (commented on by Scheraga) is suspect, at $\gamma/D = 60$.

Finally, it is of interest to reinterpret the shear-thinning phenomenon as a temperature dependence of the effective viscosity at a constant shear. If the temperature variations of the ambient fluid are sufficiently small, then the suspension could actually show an increase of the effective viscosity with temperature because D increases. Alternatively, addition of rigid particles with a suitable distribution of aspect ratios could, in principle, be used as a way of producing lubricating oils with viscosities which are independent of ambient temperature.

Acknowledgement is made to the donors of the Petroleum Research fund, administered by the American Chemical Society, for partial support of L. G. L.

REFERENCES

Batchelor, G. K. 1970 *J. Fluid Mech.* **41**, 545.

Boeder, P. 1932 *Z. Phys.* **75**, 258.

Brenner, H. 1972 *Progress in Heat and Mass Transfer*, vol. 5. (ed. by N. F. Afgan, A. V. Luikov, W. J. Minkowycz and W. R. Schowalter). Pergamon Press.

Bretherton, F. P. 1962 *J. Fluid Mech.* **14**, 284.

Burgers, J. M. 1938 *Kon. Ned. Akad. Wet. Verhand (Eerste Sedic)*, **16**, 113.

Chaffey, C. E., Takano, M. & Mason, S. G. 1965 *Can. J. Phys.* **43**, 1269.

Giesekus, H. 1962 *Rheol. Acta*, **2**, 50.

Jeffery, G. B. 1922 *Proc. Roy. Soc.* A **102**, 161.

Kirkwood, J. G. & Auer, P. L. 1951 *J. Chem. Phys.* **19**, 281.

Leal, L. G. 1971 *J. Fluid Mech.* **46**, 395.

LEAL, L. G. & HINCH, E. J. 1971 *J. Fluid Mech.* **46**, 685.

PETERLIN, A. 1938 *Z. Phys.* **112**, 1.

PRAGER, S. 1957 *Trans. Soc. Rheol.* **1**, 53.

SADRON, C. 1953 Chap. 4 of *Flow properties of Disperse Systems* (ed. J. J. Hermans). North-Holland.

SAITO, N. 1951 *J. Phys. Soc. Japan*, **6**, 297.

SCHERAGA, H. A. 1955 *J. Chem. Phys.* **23**, 1526.

TAKSERMAN-KROZER, R. & ZIABICKI, A. 1963 *J. Polymer Sci.* **1**, 491.